Pharmaceutical Sciences Asia

Pharm Sci Asia 2026; 53(3), 419-429

DOI:10.29090/psa.2026.03.26.12641

Research Article

Amorphous solid dispersion of diosmetin prepared by hot melt extrusion: Processability, stability and dissolution behavior

Padson Danraharn [1], Vipaporn Sareedenchai [2], Thanu Thongnopkoon [3*]

[1] Faculty of Pharmacy, Srinakharinwirot University, Nakhon Nayok, Thailand
[2] Department of Pharmacognosy, Faculty of Pharmacy, Srinakharinwirot University, Nakhon Nayok, Thailand
[3] Department of Pharmaceutical Technology, Faculty of Pharmacy, Srinakharinwirot University, Nakhon Nayok, Thailand

ABSTRACT

Diosmetin (DM) is a natural flavonoid with poor water solubility and low bioavailability. This study aimed to improve the dissolution of DM by preparing amorphous solid dispersions (ASDs) using hot melt extrusion (HME) with chitosan lactate (CL) and polyvinylpyrrolidone K30 (PVP-K30). The processability of the formulations was evaluated during extrusion, while the extrudates were characterized for thermal behavior, crystallinity, intermolecular interaction, drug content, physical stability, and *in vitro* dissolution in simulated gastric fluid (pH 1.2) and phosphate buffer (pH 6.8). Thermal behaviors and PXRD diffractograms confirmed the transformation of crystalline DM into the amorphous form after HME, while Fourier Transform Infrared Spectroscopy (FT-IR) suggested intermolecular interactions between DM and the polymer matrix, contributing to stabilization of the amorphous form. The ASDs showed acceptable drug content and remained physically stable after storage for 30 days. The ASDs exhibited formulation dependent and pH-dependent dissolution profiles, with only certain formulations showing improved DM dissolution compared with crystalline DM. Rapid hydration and gel formation of CL could be observed and they promoted particle agglomeration and hindered drug diffusion from the polymer matrix. These findings indicate that the dissolution performance of CL/PVP-K30-based ASDs is governed by the balance between the amorphization and the dissolution retarding effects of polymer hydration, highlighting the importance of polymer selection for optimizing HME formulations of poorly water-soluble drugs.

Keywords:
Diosmetin; Hot melt extrusion; Amorphous solid dispersion; Chitosan lactate

1. INTRODUCTION

Hot melt extrusion (HME) is a process of compressing and transforming of powder blends, i.e. active pharmaceutical ingredient (API), polymers and additives, through an orifice under the controlled parameters, including temperature, pressure, screw speed and feeding rate, to form a uniformly shaped extrudate [1,2]. HME is an effective and widely used technique in the manufacture of pharmaceutical solid products, e.g. solid dispersions, drug complexes, cocrystals, due to its numerous advantages, particularly its one-step and continuous process with the absence of solvents [2,3]. Additionally, HME can provide a product with acceptable stability and homogeneous distribution of API. A major limitation of HME is that it requires a certain high temperature in the process, which can affect the thermal stability of API and carriers being processed. The temperature of the process can be lowered by adding a plasticizer that reduces the glass transition temperature (T_g) of the polymer, resulting in the easier processability. Some plasticizers used in

***Corresponding author:**
* Thanu Thongnopkoon Email: thanu@g.swu.ac.th

HME include triacetin, triethyl citrate, acetyl tributyl citrate, propylene glycol, glycerin, dibutyl sebacate, glyceryl behenate and polyethylene glycol [4]. HME has been used to fabricate the pharmaceutical products both to increase the dissolution rate and to control the drug release as desired based on the polymer used. Polymers have a significant effect on the properties of the products prepared by HME [5]. They play a critical role in stabilizing the amorphous behavior and preventing drug recrystallization. During HME process, the polymer melts at a temperature above its T_g and acts as a binder of the system. The drug is closely mixed with the molten polymer and then embedded in the polymer matrix. Polymers having T_g below the drug degradation temperatures should be selected to prevent the API degradation. The various polymers used in HME include polyethylene glycol (PEG), polyethylene oxide (PEO), hydroxypropyl cellulose (HPC), hydroxypropyl methylcellulose (HPMC), ethyl cellulose (EC), polyvinylpyrrolidone (PVP), polyvinyl acetate (PVA) and synthetic copolymers derived from esters of acrylic and methacrylic acid (Eudragit®). HME extrudates containing *Scutellariae baicalensis radix* extract and chitosan with HPMC as a polymer exhibited the improved release of baicalin, a poorly water-soluble bioactive compound but the use of higher ratio of HPMC resulted in the slower release of baicalin [6]. HME extrudates of amorphous solid dispersions containing 25%w/w ibuprofen with Eudragit EPO were prepared and it was found that Compritol 888 ATO added as a plasticizer did not mix with the systems, remaining in the crystalline phase and showing a slower drug release when introduced into tablet formulations [7]. HME extrudates of piperine with various polymers, namely Eudragit EPO, Kollidon® VA 64 or Soluplus® were prepared using a twin-screw extruder and the results showed that hydrogen bonding can be detected only in the extrudates containing Soluplus® which hence showed the markedly enhanced dissolution rate and solubility of piperine [8].

Diosmetin (DM) is a natural flavonoid compound found in various herbs, vegetables and fruits including oranges and lemons [9]. It is an aglycone of diosmin which is a drug with a protective effect on blood vessels. DM has been studied and documented a number of pharmacological activities, e.g. antioxidant, anti-inflammatory, cardioprotective and anticancer activities. DM also shows the potential against influenza-related diseases and SARS-CoV-2 virus infections. However, the clinical application of DM is limited by poor aqueous solubility, resulting in low dissolution rate and consequently low oral bioavailability. DM has been processed through several techniques to improve its dissolution, e.g. soy lecithin based phytosome and solid self-microemulsifying drug delivery system by electrospray [10,11]. Chitosan lactate (CL), a water-soluble derivative of chitosan, possesses favorable properties including biocompatibility, biodegradability, bioadhesion, aqueous solubility, and low toxicity [12]. However, CL is not commonly used in HME process. In this study, amorphous solid dispersions (ASDs) of DM were prepared using a co-rotating twin-screw extruder with various carrier systems, i.e. CL and PVP-K30 as polymer matrices, PEG6000 and poloxamer188 (PLX) as plasticizers, in order to investigate the efficiency of carriers to improve the dissolution behavior of DM. The prepared formulations were physically characterized using differential scanning calorimetry (DSC), Fourier Transform Infrared Spectroscopy (FT-IR), Powder X-ray Diffraction (PXRD), dissolution behavior and physical stability.

2. MATERIALS AND METHODS

2.1. Materials

Diosmetin (DM) (98% purity) and chitosan lactate (CL) were purchased from MySkinRecipes® (Bangkok, Thailand). Polyvinylpyrrolidone K30 (PVP-K30) and polyethylene glycol 6000 (PEG6000) were bought from P.C. drug center (Bangkok, Thailand). Poloxamer 188 (PLX) was obtained from Merck KGaA (Darmstadt, Germany).

2.2. Preparation of ASD by hot melt extrusion

ASDs containing DM were prepared using a co-rotating twin screw hot melt extruder (HAAKE™ MiniLab 3 Micro Compounder, Thermo Fisher Scientific, Karlsruhe, Germany). DM (10% by weight of the systems), CL, PVP-K30, and the plasticizers (PEG6000 or PLX), were weighed according to the compositions listed in Table 1 and premixed using a mortar and pestle to obtain the evenly distributed samples prior to processing. The premixed samples were processed by hot melt extrusion at 120˚C and a screw speed of 20 rpm. Under the influence of heat and shear forces generated within the extrusion barrel, DM was dispersed throughout the carrier matrix to form solid dispersion systems. The extrudates were collected at the die outlet, cooled by leaving at room temperature, and subsequently stored in a desiccator before characterizations.

2.3. Differential Scanning Calorimetry (DSC)

Thermal behavior of unprocessed excipients, physical mixtures (PM), and ASDs was characterized using a differential scanning calorimeter (DSC 5+, Mettler Toledo, Greifensee, Switzerland). Each sample was accurately weighed (2-5 mg) and sealed in an aluminum pan. Thermal analyses were conducted under

Table 1. Compositions of ASDs of DM.

Ingredients	Concentration (% by weight)				
	S1	**S2**	**S3**	**S4**	**S5**
Diosmetin (DM)	10	10	10	10	10
Chitosan lactate (CL)	35	35	45	0	0
PVP-K30	35	35	45	70	70
Poloxamer188 (PLX)	20	0	0	20	0
PEG6000	0	20	0	0	20

a nitrogen purge at a flow rate of 50 mL/min. Samples were heated from 30 to 300 °C with a heating rate of 10 °C/min. Thermograms were evaluated to determine thermal behaviors and to investigate the physical state of DM by STARe software.

2.4. Powder X-ray Diffraction (PXRD)

Powder X-ray Diffraction (PXRD) analysis was performed to investigate the crystallinity of the prepared formulations. Diffractograms of the unprocessed excipients, PMs, and ASDs were obtained using a D2 PHASER benchtop X-ray diffractometer (Bruker AXS, Germany) equipped with a Cu-Kα radiation source (λ = 1.5406 Å). Measurements were conducted at an operating voltage of 30 kV and a current of 10 mA. Samples were scanned over a diffraction angle (2θ) range of 5–40˚ with a step increment of 0.02˚ and an acquisition time of 0.5 s per step.

2.5. Fourier Transform Infrared Spectroscopy (FT-IR)

Fourier Transform Infrared Spectroscopy (FT-IR) was used to examine intermolecular interactions between DM and the other components. The spectra were recorded using FT-IR spectrometer (Frontier, PerkinElmer, Liantrisant, UK) over the wavenumber range of 4000–500 cm^{-1}. Prior to analysis, the ASD samples were milled and sieved through No.40 mesh (425 µm) to obtain uniform powders.

2.6. *In vitro* dissolution study

The dissolution behavior of DM from the prepared formulations was evaluated using a USP Apparatus II (paddle method) dissolution tester (Agilent 708-DS Dissolution Apparatus, Agilent Technologies, Santa Clara, CA, USA). Extrudates were milled and passed through a No. 40 sieve (425 µm) prior to testing. Samples equivalent to 50 mg of DM were introduced into 900 mL of dissolution medium maintained at 37±0.5 °C. Dissolution studies were conducted in both simulated gastric fluid (pH 1.2) and phosphate buffer (pH 6.8) to assess the release performance under gastrointestinal conditions. The paddle speed was set at 50 rpm throughout the experiment. At predetermined intervals (0, 5, 10, 15, 20, 30, 45, 60, 90, and 120 min), 15 mL aliquots were withdrawn and immediately replaced with an equal volume of fresh dissolution medium maintained at the same temperature. The collected samples were analyzed using a UV–visible spectrophotometer (UV-2600, Shimadzu, Kyoto, Japan) at 348 nm. The cumulative percentage of DM released was calculated and plotted as a function of dissolution time.

2.7. Diosmetin content in ASDs

The DM content in ASDs was determined using UV–visible spectrophotometry. The finely ground extrudates were accurately weighed to obtain the equivalent weight of DM for 2.5 mg and transferred into a 25 mL volumetric flask. A mixture of absolute ethanol and pH 6.8 phosphate buffer (7:3) was added to dissolve DM and sonicated until a clear solution was obtained. Then, 1 mL aliquot was transferred into a 10 mL volumetric flask and diluted to volume with the same solvent mixture. The absorbance was measured at 348 nm using a UV–visible spectrophotometer (UV-2600, Shimadzu, Kyoto, Japan). The percentage drug content of each sample was calculated according to Equation (1). All analyses were performed in triplicate, and the results were expressed as mean ± standard deviation.

$$\text{Drug Content (\%)} = \frac{\text{Amount of DM determined experimentally}}{\text{Theoretical amount of DM}} \times 100 \quad (1)$$

2.8. Stability study

To evaluate the physical stability of ASDs, the extrudates were milled and sieved through a No. 40 mesh (425 µm). Then the samples were kept in glass vials sealed with perforated parafilm and stored under two different storage conditions: accelerated conditions at 40˚C/75% relative humidity (RH) and room temperature (RT)/75% RH. All samples were stored for 30 days before characterization by PXRD with the aforementioned conditions.

Figure 1. Appearances of DM ASDs prepared by hot melt extrusion; S1 (top), S2 (middle) and S3 (bottom).

3. RESULTS AND DISCUSSION

3.1. Preparation of ASDs of DM by hot melt extrusion

Five formulations of DM ASDs were prepared using HME at the same processing conditions but among the five formulations, only S1–S3, which contained CL, were successfully processed into continuous cylindrical extrudates (Figure 1). The measured torque values during extrusion were approximately 1.70, 1.51, and 2.13 Nm for S1, S2, and S3, respectively. In contrast, the formulation S4 and S5, which did not contain CL, generated considerably higher torque values of approximately 3.04 and 3.37 Nm. Although these values remained below the maximum torque capacity of the laboratory scale extruder (5 Nm), the extrusion process was discontinued because the rapidly increasing torque indicated substantially greater melt resistance and could impose excessive mechanical load on the instrument. Torque is an important processing parameter in HME because it reflects the resistance of the molten material to screw rotation and is closely related to melt viscosity and processability [13]. Formulations containing CL (S1–S3) exhibited considerably lower torque values than formulations without CL (S4–S5), suggesting that CL improved melt processability during extrusion. Although PEG6000 and PLX are commonly used as plasticizer but S3, which contained neither additive, was successfully extruded. These results suggest that CL can improve processability under the present processing conditions [14,15]. However, the underlying mechanism requires further rheological investigation. Figure 1 shows the appearance of the successfully extruded formulations. All formulations formed continuous cylindrical strands with relatively smooth surfaces. S3 exhibited a darker brown extrudate than S1 and S2. Although all formulations were produced under the identical process conditions, S3 showed the highest torque among the successfully extruded formulations, indicating greater melt resistance. During HME, mechanical work is generated by screw rotation and shear contributes. Therefore, the darker extrudate of S3 may be associated with greater thermomechanical stress during processing [16].

3.2. Differential Scanning Calorimetry (DSC)

As shown in Figure 2A, pure DM exhibited a sharp endothermic peak at 262.50˚C, corresponding to its melting temperature (T_m), which is characteristic of its crystalline form. Similar melting temperatures have been reported for diosmetin in previous studies, where the melting endotherm was observed in the range of approximately 255–264˚C, confirming the crystallinity of the compound [17,18]. PEG exhibited a sharp endothermic peak at 64.67˚C and PLX displayed a melting endotherm at 54.83˚C, corresponding to the melting of their semi-crystalline nature. In contrast, PVP-K30 did not exhibit a melting endotherm but showed a baseline shift with a glass transition temperature (T_g) of approximately 162.64˚C. The absence of a melting peak confirms the amorphous nature of PVP, while the observed T_g is consistent with K-values [19]. The DSC thermogram of CL exhibited a broad thermal transition between 70 and 220˚C with a weak endothermic event centered around 190˚C. Similar thermal behavior has been reported for chitosan-based materials, where broad transitions are often attributed to polymer chain relaxation and moisture-related thermal events rather than a true T_g, as the T_g of chitosan is believed to be obscured by thermal degradation occurring at higher temperatures [20,21]. The absence of a sharp melting endotherm suggests that CL exists in an amorphous state.

The DSC thermograms of the extruded samples were shown in Figure 2B. The absence of T_m of

crystalline DM suggests that detectable crystalline DM was markedly reduced or DM was molecularly dispersed within the carrier matrices. However, the absence of the DM melting peak was also observed in the physical mixtures (PM). This may be because DM may dissolve in the carrier phase during DSC heating process before reaching its melting temperature. In addition, the low drug loading and the broad thermal transitions of CL may reduce the detectability of the DM melting endothermic peak. Therefore, the DSC results should be interpreted together with PXRD data to confirm the reduction in crystallinity or amorphous conversion of DM. The formulations containing PLX and PEG6000 (S1 and S2) exhibited endothermic peaks at approximately 55 and 60˚C, respectively, corresponding to the T_m of the individual carriers. The persistence of these thermal events in ASDs suggests that PLX and PEG6000 retained their semi-crystalline characteristic after HME processing and were not completely converted into an amorphous state.

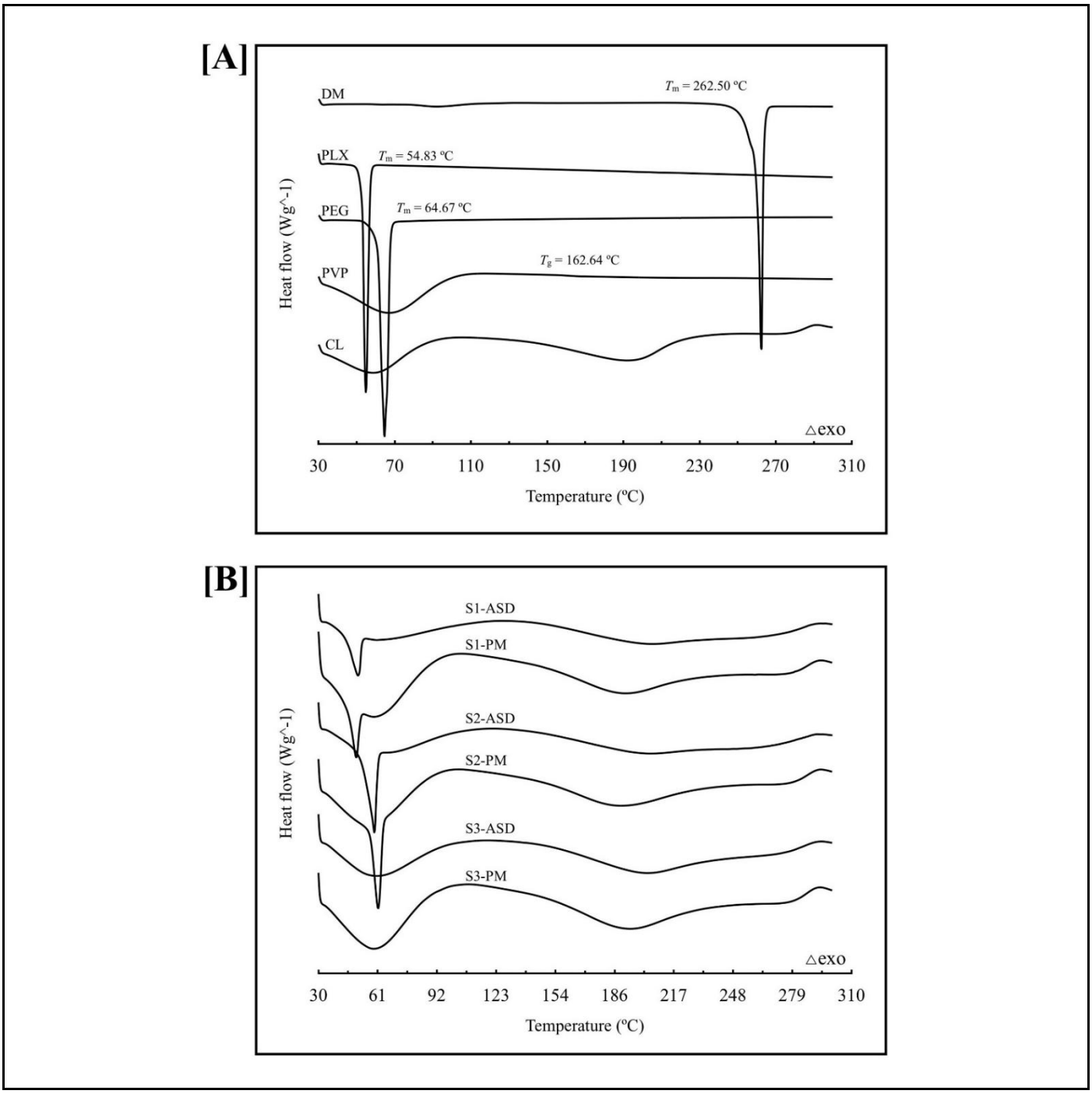

Figure 2. DSC thermograms of [A] unprocessed materials: diosmetin (DM), Poloxamer 188 (PLX), polyethylene glycol 6000 (PEG), polyvinylpyrrolidone K30 (PVP-K30), and chitosan lactate (CL); and [B] amorphous solid dispersions (ASDs) and their corresponding physical mixtures (PMs).

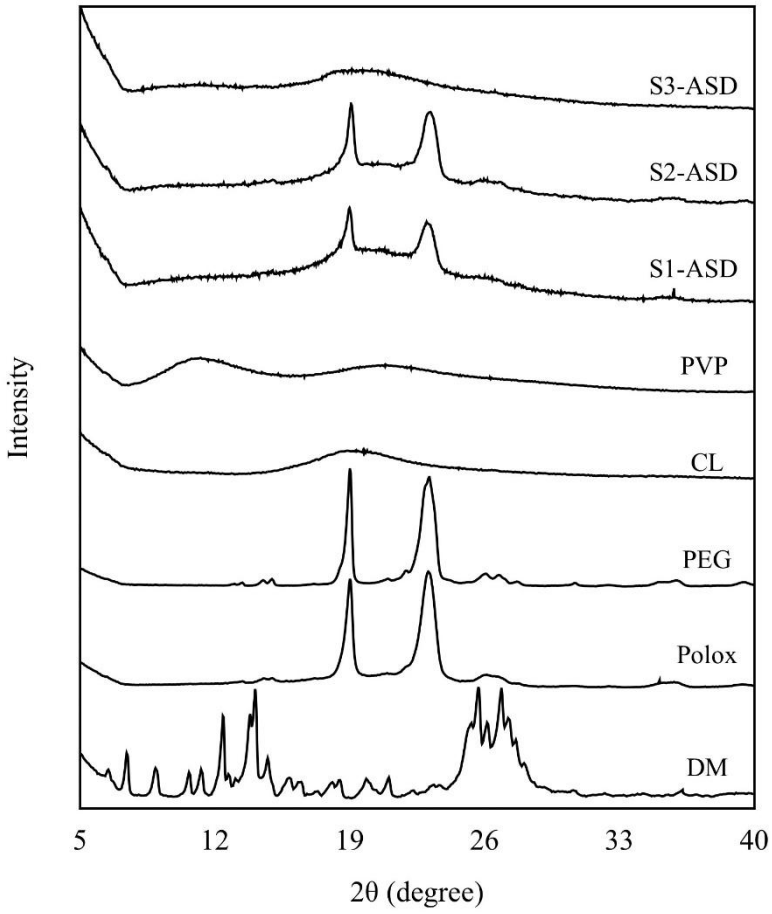

Figure 3. PXRD diffractograms of DM, unprocessed ingredients and ASDs prepared by hot melt extrusion.

3.3. Powder X-ray Diffraction (PXRD)

The diffractograms of DM, CL, PVP-K30, PEG6000, PLX, and the ASDs are presented in Figure 3. DM exhibited several diffraction peaks at approximately 12.42˚, 13.84˚, 14.09˚, 25.69˚ and 26.88˚ (2θ), confirming its crystalline form [22]. In contrast, CL and PVP-K30 exhibited broad halo patterns without diffraction peak, indicating their amorphous characteristics. PEG6000 and PLX displayed characteristic peaks at approximately 19˚ and 23˚ (2θ), consistent with their semi-crystalline structures. Regarding HME extrudates, the characteristic peaks of crystalline DM disappeared in all ASDs (S1-S3), indicating that DM was successfully converted into an amorphous form within the polymer matrices. However, S1-ASD and S2-ASD retained characteristic peaks at approximately 19˚ and 23˚ (2θ). These peaks correspond to the characteristic peaks of PEG6000 and PLX, which are known to recrystallize during cooling after melt processing [23,24]. In contrast, S3-ASD exhibited only a broad halo pattern with no detectable sharp peaks over the scanned range, indicating the absence of crystalline components in the sample. Since S3 contained neither PEG nor PLX, the absence of DM diffraction peaks further supports the successful amorphization of DM after HME processing.

3.4. Fourier Transform Infrared Spectroscopy (FT-IR)

The FT-IR spectra of the raw materials, physical mixtures (PMs), and ASDs are presented in Figure 4A. DM exhibited characteristic bands corresponding to the stretching vibration of phenolic hydroxyl (OH) groups at approximately 3536 cm^{-1}, the carbonyl (C=O) stretching vibration at 1651 cm^{-1}, aromatic C=C stretching vibrations at 1606 and 1580 cm^{-1}, and C–O stretching vibrations at 1034 cm^{-1}, which are consistent with the characteristic functional groups of flavonoids [18,25]. CL exhibited a broad band in the region of 3400 cm^{-1} attributed to O–H/N–H stretching [26], while PVP-K30 showed a characteristic carbonyl stretching band at approximately 1648 cm^{-1} [24]. Compared with DM and the corresponding PMs, the ASD formulations exhibited a markedly broader band in the 3200–3600 cm^{-1} region, accompanied by the disappearance or reduction of the OH band of DM (Figure 4B). In addition, slight changes in the region around 1500–1650 cm^{-1} were observed.

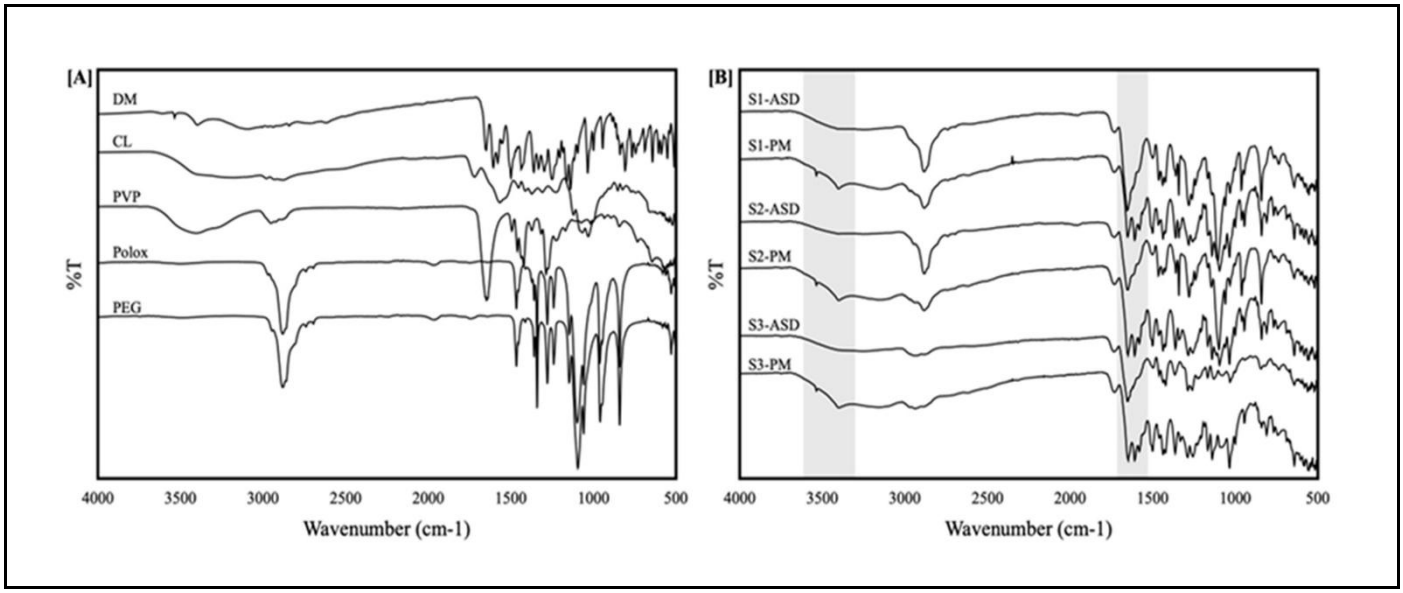

Figure 4. FT-IR spectra of unprocessed ingredients (A), physical mixtures and ASDs of DM prepared by hot melt extrusion (B).

These spectral changes suggest the formation of intermolecular hydrogen bonding between the OH groups of DM and the C=O groups of PVP and/or the amino groups of CL in the HME extrudates. Furthermore, several characteristic bands in the region around 1600–1000 cm^{-1} exhibited decreased intensity and broader band shapes in the ASDs compared with the corresponding PMs. This is associated with the conversion of crystalline form into amorphous form, where the loss of long-range molecular order results in a distribution of molecular conformations and molecular environments, leading to broader and less intensity of bands. These findings are consistent with the DSC and PXRD results, which confirmed the amorphization of DM after HME [27].

3.5. *In vitro* dissolution study

The dissolution profiles of DM and ASDs in pH 1.2 buffer and pH 6.8 phosphate buffer are shown in Figure 5. HME processing resulted in modest improvements in drug dissolution despite the amorphization of DM confirmed by DSC and PXRD. This finding suggests that factors other than the solid-state transformation influenced the dissolution behavior of the formulations.

ASDs rapidly formed compact agglomerates upon contact with the dissolution medium, as shown in Figure 6. The formation of these cohesive masses likely reduced the effective surface area available for dissolution and hindered penetration of the dissolution medium into the polymer matrix. CL is known to readily absorb water and form a hydrated gel layer during hydration. This gel forming property, together with the cohesive polymer network provided by PVP, may promote the formation of dense agglomerates that further restricted medium penetration and drug diffusion from the interior of the matrix. Consequently, drug release was limited despite successful amorphization. Similar behavior has been reported for polymeric ASD systems, where polymer hydration and matrix formation reduce water penetration and retard drug diffusion despite improved apparent solubility [28-30].

In pH 1.2 buffer, S2 exhibited lower drug release than DM, whereas S1 and S3 showed only slight improvements during the early stage. The reduced dissolution of S2 was likely associated with the formation of dense agglomerates shown in Figure 6A, which limited medium penetration and drug diffusion. In pH 6.8 phosphate buffer, S2 demonstrated the highest drug release, while S1 showed the lowest dissolution behavior. This corresponded with visual observations which showed that S1 formed the largest and most compact agglomerates shown in Figure 6B, whereas S2 formed fewer compact aggregates, allowing greater access of the dissolution medium. In addition, the dissolution samples withdrawn from the pH 1.2 study became slightly turbid after standing at room temperature during the later sampling intervals (60-120 min). Although precipitation was not directly confirmed, this observation may indicate precipitation of supersaturated DM after cooling. The decrease in temperature could reduce the solubility of DM, leading to precipitation from a supersaturated state. Similar supersaturated precipitation behavior has been widely described for ASDs, in which rapid dissolution initially generates supersaturation, followed by precipitation when supersaturation cannot be maintained [31]. These results indicate that although HME successfully converted crystalline DM into an amorphous form, the dissolution performance might be influenced by formulation behavior during hydration.

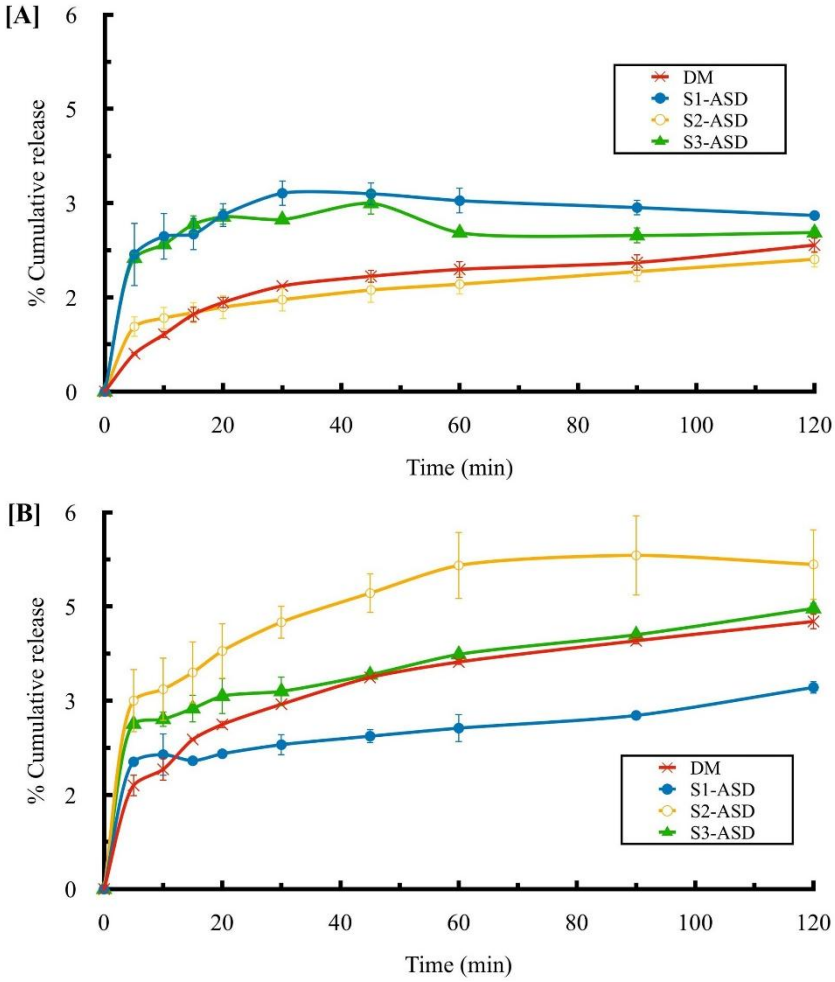

Figure 5. Dissolution profiles of DM and ASDs of DM prepared by hot melt extrusion : [A] in pH 1.2 buffer and [B] in pH 6.8 phosphate buffer.

The formation of compact agglomerates limited water penetration and drug diffusion, thereby restricting the expected enhancement in dissolution. Therefore, reducing particle agglomeration and improving matrix disintegration may be important considerations for further optimizing the formulation. The higher dissolution of DM in pH 6.8 phosphate buffer compared with pH 1.2 buffer may also be due to the DM solubility increasing with higher pH, which is consistent with previous studies [32,33].

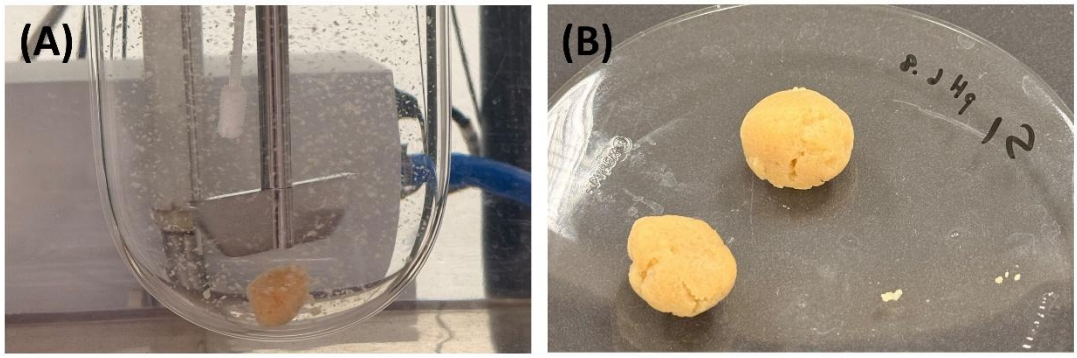

Figure 6. Appearances of ASD during and after dissolution studies, especially for the samples containing CL. (A) S2-ASD in pH 1.2 buffer and (B) S1-ASD in pH 6.8 phosphate buffer.

Table 2. Diosmetin content in ASDs prepared by hot melt extrusion.

Sample	Content (%) ± SD
S1-ASD	102.21 ± 3.24
S2-ASD	100.56 ± 2.13
S3-ASD	104.37 ± 1.13

3.6. Diosmetin content in ASDs

The DM content values in all ASDs were close to the theoretical content (100%) as displayed in Table 2. These results suggest that the HME process did not cause drug degradation or loss and ensured uniform incorporation of DM into the polymer matrices. The low variability among replicates also indicates desirable content uniformity, supporting the reliability of the ASDs for subsequent physicochemical characterizations and dissolution studies.

3.7. Stability study

The physical stability of the ASDs was evaluated after storage for 30 days under two conditions (40˚C/75% RH and RT/75% RH) and the results are displayed in Figure 7. The PXRD diffraction patterns obtained after storage were compared with initial samples to determine whether recrystallization occurred during storage. For S1 and S2, the characteristic diffraction peaks remained at the same 2θ positions after storage under both conditions, and no additional diffraction peak or significant peak shift was observed. Although slight variations in peak intensity were detected, these changes are most likely attributable to differences in sample packing, preferred orientation, or instrumental factors rather than changes in the crystalline state [34]. Therefore, the PXRD results indicate that no detectable recrystallization occurred during the storage period. S3 exhibited a broad halo pattern in the initial, confirming its amorphous form. This halo was preserved after storage under both 40˚C/75% RH and RT/75% RH without the appearance of new diffraction peaks, indicating that no measurable recrystallization occurred during the study period. The physical stability observed in all formulations might be attributable to the intermolecular interactions between DM and polymers as characterized by FT-IR. According to FT-IR spectra, the disappearance of the OH band of DM suggested the formation of intermolecular hydrogen bonding between DM and the carrier matrix. Such drug–polymer interactions are known to reduce molecular mobility,

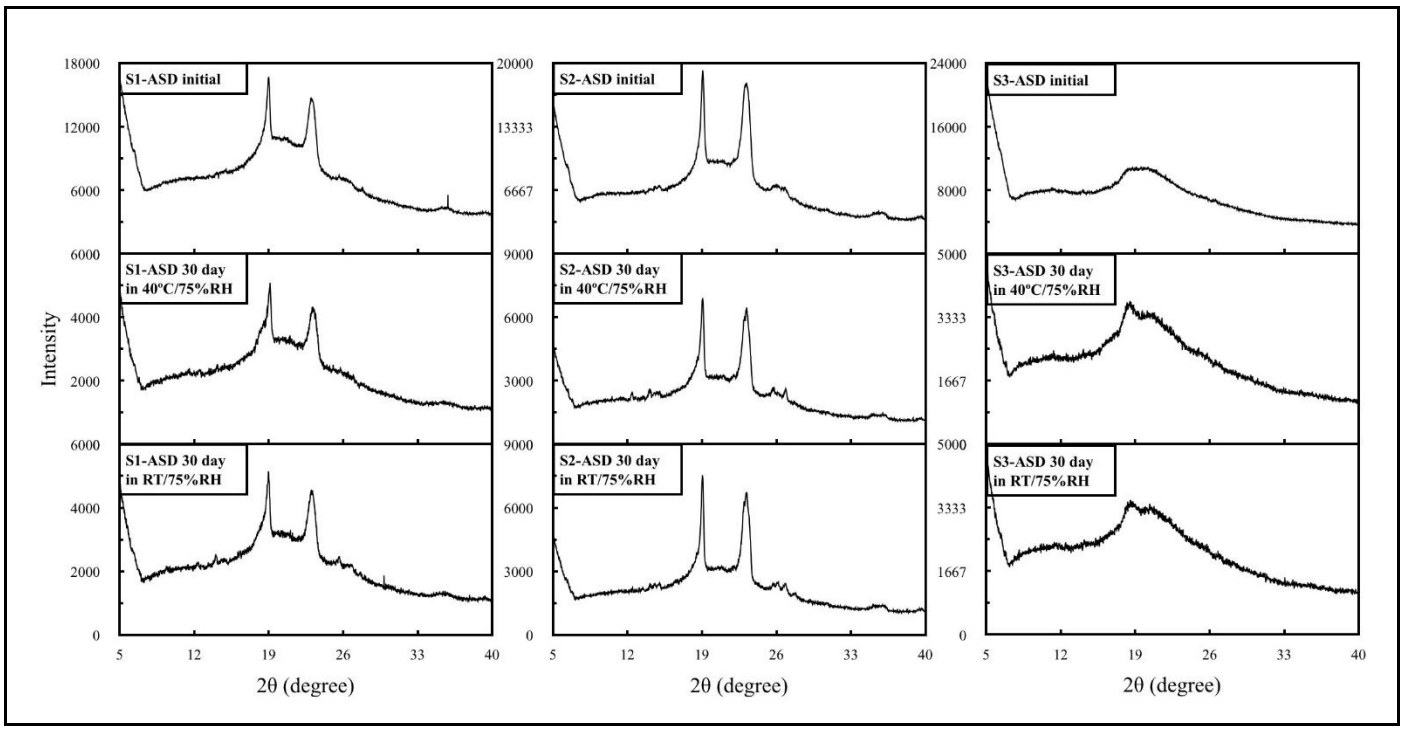

Figure 7. PXRD diffractograms of ASDs (S1, S2, S3) before and after storage under two conditions, i.e. 40˚C/75% RH and RT/75% RH, for 30 days.

restrict molecular rearrangement, and consequently suppress nucleation and crystal growth, thereby improving the physical stability of ASDs. The absence of new diffraction peaks after storage is therefore consistent with the stabilizing effect of these intermolecular interactions [35,36].

4. CONCLUSIONS

ASDs of DM were successfully produced by HME with using CL and PVP blend as a carrier, which contributed to maintaining the amorphous state and improving the physical stability of the formulations during storage. Among the investigated formulations, the combination of CL and PVP resulted in the successful extrusion without the need of additional plasticizers, indicating that CL played an important role in improving processability. This finding suggests that CL can function not only as a polymeric carrier but also as a processing aid for HME. Dissolution studies demonstrated formulation dependent and pH-dependent dissolution profiles, with some ASD formulations showing improved DM release compared with crystalline DM. However, the present study also revealed that dissolution performance was governed not only by amorphization, but also by the balance between dissolution promoting mechanisms and dissolution retarding mechanisms arising from gel formation and agglomeration caused by the polymer used. In particular, the hydration and gel forming ability of CL promoted the formation of cohesive agglomerates and limited water penetration into the matrix, thereby offsetting the dissolution advantage of the amorphous state. Overall, these findings indicate that successful ASD formulation should consider not only the ability to generate and stabilize the amorphous form, but also the matrix forming behavior of the polymer during dissolution. This concept provides an important consideration for the selection of polymer systems in future HME formulations.

5. ACKNOWLEDGEMENTS

The authors are thankful to the Faculty of Pharmacy, Srinakharinwirot University for providing the facility and equipment.

Author contribution

P.D.: Methodology, Data collection, Data curation, Formal analysis, Investigation, Writing-original draft preparation. V.S.: Conceptualization, Methodology, Supervision. T.T.: Conceptualization, Methodology, Supervision, Writing-original draft preparation, Writing – review and editing.

Funding

None to declare.

Conflict of interest

None to declare.

Ethics approval

None to declare.

Article info*:*

Received July 31, 2026
Received in revise form August 25, 2026
Accepted August 26, 2026

REFERENCES

1. Essa E, Amin M, Sultan A, Arafa M, El Maghraby G, McConville C. Hot melt extrusion for enhanced dissolution and intestinal absorption of hydrochlorothiazide. J Drug Deliv Sci Technol. 2023;88:104895.
2. Patil H, Vemula SK, Narala S, Lakkala P, Munnangi SR, Narala N, et al. Hot-Melt Extrusion: from theory to application in pharmaceutical formulation - Where are we now? AAPS PharmSciTech. 2024;25:37. doi: 10.1208/s12249-024-02749-2.
3. Mannala T. Hot melt extrusion: A viable option for implementing continuous manufacturing in the pharmaceutical industry. JDDT. 2025;15(10):87-97.
4. Desai D, Sandhu H, Shah N, Malick W, Zia H, Phuapradit W, et al. Selection of solid-state plasticizers as processing aids for hot-melt extrusion. J Pharm Sci. 2018;107(1):372-79.
5. Jagtap PS, Jain SS, Dand N, Jadhav KR, Kadam VJ. Hot melt extrusion technology, approach of solubility enhancement: A brief review. Der Pharmacia Lettre. 2012;4(1):42-53.
6. Paczkowska-Walendowska M, Miklaszewski A, Szymanowska D, Skalicka-Wozniak K, Cielecka-Piontek J. Hot melt extrusion as an effective process in the development of mucoadhesive tablets containing *Scutellariae baicalensis* radix extract and chitosan dedicated to the treatment of oral infections. Int J Mol Sci. 2023;24:5834. doi: 10.3390/ijms24065834.
7. Biedrzycka K, Marcinkowska A. The use of hot melt extrusion to prepare a solid dispersion of ibuprofen in a polymer matrix. Polymers. 2023;15:2912. doi: 10.3390/polym15132912.
8. Ashour EA, Majumdar S, Alsheteli A, Alshehri S, Alsulays B, Feng X, et al. Hot melt extrusion as an approach to improve solubility, permeability and oral absorption of a psychoactive natural product, piperine. J Pharm Pharmacol. 2016;68:989-98.
9. Wujec M, Feldo M. Can we improve diosmetin activity? The State-of-the-Art and promising research directions. Molecules. 2023;28:7910. doi: 10.3390/molecules28237910.
10. Huynh TKC, Duong BN, Ho BT, Nguyen HP, Ton AK, Nguyen TCT, et al. Enhanced solubility and *in vitro* drug release of diosmetin from soy lecithin based-diosmetin phytosome. Vietnam J Chem. 2024;1–12. doi: 10.1002/vjch.202300326.
11. Gu Z, Xue Y, Li S, Adu-Frimpong M, Xu Y, Yu J, et al. Design, characterization, and evaluation of diosmetin-loaded solid self-microemulsifying drug delivery system prepared by electrospray for improved bioavailability. AAPS PharmSciTech. 2022;23(4):106. doi: 10.1208/s12249-022-02263-3.
12. Arpa MD, Erim ÜC, Kesmen Salik EE, Kaleli SNB, Erol I. Effect of organic acid selection on the physicochemical properties, bioadhesion, and stability of chitosan hydrogels. Gels. 2025;11:778. doi: 10.3390/gels11100778.
13. Censi R, Gigliobianco MR, Casadidio C, Di Martino P. Hot melt extrusion: Highlighting physicochemical factors to be investigated while designing and optimizing a hot melt extrusion process. Pharmaceutics. 2018;10:89. doi: 10.3390/pharmaceutics10030089.

14. Meng Q, Heuzey MC, Carreau PJ. Hierarchical structure and physicochemical properties of plasticized chitosan. Biomacromolecules. 2014;15(4):1216–24.
15. Jeung S, Mishra MK. Hot melt reactive extrusion of chitosan with poly(acrylic acid). Int J Polym Mater Polym Biomater. 2010;60:102-13.
16. Li S, Tian Y, Jones DS, Andrews GP. Optimising drug solubilisation in amorphous polymer dispersions: Rational selection of hot-melt extrusion processing parameters. AAPS PharmSciTech. 2016;17(1):200-13. doi: 10.1208/s12249-015-0450-6.
17. Brad K, Chen C. Physicochemical properties of diosmetin and lecithin complex. Trop J Pharm Res. 2013;12(4):453-56.
18. Sheoran S, Arora S, Singh H, Kumar A, Vuree S, Vancha H, et al. Characterization, development and validation of UV Spectrophotometric technique for determining Diosmetin in bulk and nanoformulations. Results Chem. 2023;2:100972.
19. Hancock BC, Zografi G. Characteristics and significance of the amorphous state in pharmaceutical systems. J Pharm Sci. 1997;86(1):1-12.
20. Kittur FS, Harish Prashanth KV, Udaya Sankar K, Tharanathan RN. Characterization of chitin, chitosan and their carboxymethyl derivatives by differential scanning calorimetry. Carbohydr Polym. 2002;49(2):185-93.
21. Pereira FS, da Silva Agostini DL, Job AE, González ERP. Thermal studies of chitin–chitosan derivatives. J Therm Anal Calorim. 2013;114:321-27.
22. Uniyal P, Pramanik SD, Pandey S, Shukla P, Roy P, Parashar D, et al. Synergistic combinatorial anticancer potential of tamoxifen with naringin and diosmetin in MCF-7 breast cancer cells and their liposomal delivery. Sci Rep. 2026;16:7646. doi: 10.1038/s41598-026-37954-5.
23. Kidokoro M, Sasaki K, Haramiishi Y, Matahira N. Effect of crystallization behavior of polyethylene glycol 6000 on the properties of granules prepared by fluidized hot-melt granulation (FHMG). Chem Pharm Bull (Tokyo). 2003;51(5):487-93. doi: 10.1248/cpb.51.487.
24. Fousteris E, Tarantili PA, Karavas E, Bikiaris D. Poly(vinyl pyrrolidone)-poloxamer-188 solid dispersions prepared by hot melt extrusion. J Therm Anal Calorim. 2013;113:1037-47.
25. Angamuthu H, Ramachandrane M. Investigations on the structural, vibrational, computational, and molecular docking studies on potential antidiabetic chemical agent Diosmetin. J Mol Recognit. 2019. doi: 10.1002/jmr.2819.
26. Cervera MF, Heinämäki J, de la Paz N, López O, Maunu SL, Virtanen T, et al. Effects of spray drying on physicochemical properties of chitosan acid salts. AAPS PharmSciTech. 2011;12(2):637-49. doi:10.1208/s12249-011-9620-3.
27. Kamble HA, Srinivasan G. Exploring an interplay between drug-polymer interactions and amorphous solid dispersion stability: A review. Pharm Sci Asia. 2025;52(4):442-59. doi: 10.29090/psa.2025.04. 25.3959.
28. Thakur VK, Thakur MK. Handbook of Polymers for Pharmaceutical Technologies. MA, USA: Scrivener Publishing; 2016.
29. Shi Q, Chen H, Wang Y, Wang R, Xu J, Zhang C. Amorphous solid dispersions: Role of the polymer and its importance in physical stability and *in vitro* performance. Pharmaceutics. 2022;14(8):1747. doi: 10.3390/pharmaceutics14081747.
30. Efentakis M, Stamoylis K. An investigation into the swelling properties, dimensional changes, and gel layer evolution in chitosan tablets undergoing hydration. Adv Polym Technol. 2009;28(1):32-39. doi: 10.1002/adv.20147.
31. Kong Y, Wang W, Wang C, Li L, Peng D, Tian B. Supersaturation and phase behavior during dissolution of amorphous solid dispersions. Int J Pharm. 2023;631:122524.
32. BenchChem Technical Support Team. Diosmetin formulation with buffering agents to improve absorption [Internet]. United States: BenchChem; 2026 [cited 2026 Aug 24]. Available from:https://www.benchchem.com/product/b1670712/docs#diosmetin-formulation-with-buffering agents-to-improve-absorption]
33. Li Y, Zhang Y, Qi M, Yi L, Yu Y, Yang W, et al. Solubility behavior of diosmetin in pure and binary solvents: Thermodynamic evaluation and molecular-level interpretation. Fluid Phase Equilib. 2026;602:114611. doi: 10.1016/j.fluid.2025.114611.
34. Bish DL, Chipera SJ. Accuracy in quantitative X-ray powder diffraction analyses. Adv X-Ray Anal. 1995;38:47-57. doi: 10.1007/978-1-4615-1797-9_5.
35. Newman A, Knipp G, Zografi G. Assessing the performance of amorphous solid dispersions. J Pharm Sci. 2012;101(4):1355-77. doi: 10.1002/jps.23031.
36. Zografi G, Newman A. Introduction to amorphous solid dispersions. In Pharmaceutical Sciences Encyclopedia. 2015. S.C.Gad (Ed.). doi: 10.1002/9780470571224.pse522.